The use of the PeakForce^{TM} quantitative nanomechanical mapping AFM-based method for high-resolution Young's modulus measurement of polymers

2011 Meas. Sci. Technol. 22 125703

(http://iopscience.iop.org/0957-0233/22/12/125703)

Meas. Sci. Technol. **22** (2011) 125703 (6pp) doi:10.1088/0957-0233/22/12/125703

The use of the PeakForce™ quantitative nanomechanical mapping AFM-based method for high-resolution Young's modulus measurement of polymers

T J Young[1], M A Monclus[1], T L Burnett[1], W R Broughton[1], S L Ogin[2] and P A Smith[2]

[1] National Physical Laboratory, Hampton Road, Teddington, TW11 0LW, UK
[2] The University of Surrey, Guildford, GU2 7XH, UK

E-mail: Tim.young@npl.co.uk

Received 13 July 2011, in final form 20 September 2011
Published 24 October 2011
Online at stacks.iop.org/MST/22/125703

Abstract
PeakForce™ quantitative nanomechanical mapping (QNM™) is a new atomic force microscopy technique for measuring Young's modulus of materials with high spatial resolution and surface sensitivity by probing at the nanoscale. In this work, modulus results from PeakForce™ QNM™ using three different probes are presented for a number of different polymers with a range of Young's moduli that were measured independently by instrumented (nano) indentation testing (IIT). The results from the diamond and silicon AFM probes were consistent and in reasonable agreement with IIT values for the majority of samples. It is concluded that the technique is complementary to IIT; calibration requirements and potential improvements to the technique are discussed.

Keywords: atomic force microscopy, polymers, PeakForce, QNM, quantitative nanomechanical mapping, Young's modulus, tapping mode, mechanical properties

(Some figures in this article are in colour only in the electronic version)

1. Introduction

The atomic force microscope (AFM), invented in the early 1980s [1, 2], is now widely considered to be the instrument of choice for analysing surfaces at the nano- or, in some cases, atomic scale. This is mainly due to the ability of the technique to measure forces and distances at a very high resolution, and to explore non-destructively different surfaces in air or vacuum with minimal sample preparation. In addition to characterizing topography, mechanical property measurements can be made by AFM-based semi-quantitative scanning techniques (i.e. force modulation [3] and tapping mode phase imaging [4]) or by more time-consuming atomic force microscopy (i.e. force-distance curves [5]).

The pulsed-force mode of AFM operation was developed in 1997. This enabled adhesion and stiffness properties to be calculated at each point on a surface more rapidly than was previously possible [6]. In this mode, the AFM cantilever is oscillated and taps the surface periodically enabling the associated force–distance curve to be measured. These curves are then analysed in real time to extract adhesion and stiffness values. The methodology for calculating the surface Young's modulus from single-point force–distance curves [7] was developed simultaneously with the pulsed-force mode, although it was not until recently that quantification of the pulsed-force mode became possible [8]. Recent developments in noise reduction, data acquisition and processing speed have allowed an AFM manufacturer (Bruker AXS, CA, USA) to develop PeakForce™ Quantitative Nanomechanical Mapping (QNM™). This is an extension of the pulsed-force mode with improved force resolution (10^{-10} N for QNM, compared to 10^{-9} N for the pulsed-force mode [8]) combined with real time

calculation of Young's modulus at each surface contact. The manufacturer claims that the technique can measure Young's moduli of materials ranging from soft gels (∼1 MPa) to rigid polymers (>20 GPa), exceeding other AFM-based techniques (e.g. HarmoniX [9]) for nanoscale material characterization.

Accurate modulus measurements are complicated by the multiple and complex force interactions that usually occur in a tip–surface contact. The most commonly used models for the calculation of Young's modulus by AFM techniques (where the predominant contact is between a spherical tip of defined radius and a flat surface) are Hertzian, Derjaguin–Muller–Toporov (DMT) and Johnson–Kendall–Roberts (JKR) [10]. In practice, the surface is rarely flat, and the tip apex may differ from an ideal sphere, leading to errors in the calculated modulus values. An additional complication is rotation (the lateral and buckling movement) of the AFM tip during cantilever deflection which produces tip–surface shear forces that are not accounted for in these models [11].

To the authors' knowledge, no independent work has considered the degree of accuracy and applicability of the PeakForce™ QNM™ technique in a systematic way. The purpose of this investigation is to evaluate PeakForce™ QNM™ as a nanomechanical mapping technique to obtain valid modulus measurements for a range of polymers. The modulus values obtained from PeakForce™ QNM™ using different probes were compared with values measured using conventional instrumented (nano) indentation testing (IIT) and with the suppliers' data.

2. Experimental methods

2.1. Materials

Table 1 shows the materials used in this study together with the suppliers' values for Young's modulus and Poisson's ratio (where Poisson's ratio data were not available, a value of 0.35 was used). Polymer surfaces were prepared by ultramicrotomy using a Leica EM UC7 ultramicrotome (Leica Microsystems GmbH Wetzlar, Germany). The temperature was controlled (between −40 °C and −140 °C) to ensure that the ultramicrotomy resulted in a brittle fracture to minimize the surface roughness. The polymeric surfaces for investigation were cut from bulk materials (as opposed to using thin films) in order to eliminate any error arising from the interaction between a thin film and the underlying substrate during indentation by either AFM nanomechanical mapping or IIT [12].

2.2. Instrumented (nano) indentation testing

IIT experiments were performed using a NanoTest instrumented indentation platform (Micro Materials Ltd). Ten indentations, separated by 50 μm to avoid interference, were performed on each sample using a Berkovich diamond indenter by applying a 20 mN force at a constant loading rate of 0.67 mN s^{-1} over 30 s; the maximum force was then held for 100 s, and then unloading was performed at a constant unloading rate of 2 mN s^{-1} over 10 s. Values of indentation moduli were then calculated from the unloading slopes using an indenter area function obtained by metrological AFM [13].

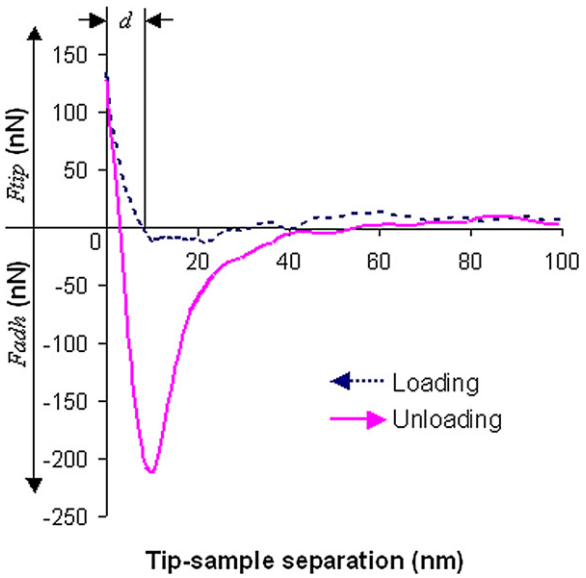

Figure 1. A force–separation curve obtained using AFM nanomechanical mapping. The loading and unloading curves have been identified along with the portions of the curve relating to the tip and adhesive forces (F_{tip} and F_{adh}, respectively).

Table 1. List of test polymers, abbreviations and the associated supplier values of Young's moduli and Poisson's ratio. Poisson's ratio values marked with an asterisk (*) are assumed values.

	Supplier Young's moduli (GPa)	Poisson's ratio
Low density polyethylene (LDPE)	0.20	0.35*
High density polyethylene (HDPE)	0.80	0.42
Acrylonitrile butadiene styrene (ABS)	2.30	0.35*
Photostress coating 1 (PS1)	2.40	0.35*
Polycarbonate (PC)	2.60	0.35*
Polyethersulfone (PES)	2.70	0.35*
Vinylester (VE)	2.70	0.38
Polyvinylidene fluoride (PVDF)	2.90	0.35*
Polystyrene (PS)	3.00	0.34
Photostress coating 8 (PS8)	3.10	0.38
Acetal (POM)	3.50	0.36
Poly(methyl methacrylate) (PMMA)	4.80	0.35*

2.3. Quantitative AFM nanomechanical mapping

2.3.1. Background theory. In PeakForce™ QNM™, Young's modulus is calculated using a DMT model (see equation (1)) that is applied to the unloading portion of the force–separation curve (see figure 1) [14]. The DMT model can be viewed as a modified Hertzian model, which takes into account the adhesive forces between the tip and the surface. According to this approach, the reduced Young's modulus, E_r, is given by

$$E_r = \frac{3(F_{tip} - F_{adh})}{4\sqrt{Rd^3}}. \quad (1)$$

In equation (1), F_{tip} is the force on the AFM tip, F_{adh} is the adhesive force between the AFM tip and sample, R is the AFM tip radius, and d is the deformation depth.

Table 2. AFM cantilevers and tips used in this study

Tip reference	Tip	Cantilever	Spring stiffness	Calculated force (required for a 2 nm deformation)	Working radius	Working applied force
Tap 525	Silicon	Silicon	97 N m^{-1}	85 nN	37 nm	120 nN
PDNISP	Diamond	Steel	227 N m^{-1}	88 nN	40 nm	500 nN
Tap190	Silicon	Silicon	56 N m^{-1}	142 nN	104 nm	238 nN

The reduced Young's modulus is related to the sample Young's modulus, E_s, by

$$\frac{1}{E_r} = \frac{\left(1-\nu_s^2\right)}{E_s} + \frac{\left(1-\nu_I^2\right)}{E_I}, \tag{2}$$

where E_I is the indenter Young's modulus, ν_I is the Poisson's ratio of the indenter and ν_s is Poisson's ratio of the sample. In this work, $E_I \gg E_s$, and so the second term on the right-hand side of equation (2) is negligible.

The tip radius can be measured directly using a scanning electron microscope or a tip calibration grating. Alternatively, the value of the radius can be derived from a reference sample (in this work, polystyrene, i.e. PS) using equation (1) and taking the modulus value to be that determined using IIT [15].

2.3.2. Instrumentation. AFM experiments were performed using a Bruker Dimension Icon AFM and three different probes: PDNISP and Tap525 probes supplied by Bruker AXS; Tap190 probes supplied by BudgetSensors™ (Innovative Solutions Bulgaria Ltd, Bulgaria). The probes (see table 2) were selected based on the recommendations of Bruker AXS for the range of polymer Young's moduli to be investigated (0.2–3.7 GPa—values based on IIT measurements). For the experiments described here, the oscillation frequency was 2 kHz and the amplitude was set at a constant value of 300 nm corresponding to an indentation rate of 1.2 mm s^{-1}. All AFM experiments were performed within a two-week period of the last IIT measurement. The probes were used sequentially for measurements on all the polymers and the polymers were kept in a desiccator (<30% RH at 21 °C) between measurements. Each set of Young's modulus measurements on a sample corresponds to 256 × 256 force–separation curves obtained over an area of 2 μm × 2 μm. These data are presented as histograms.

To optimize the experimental settings (working radius and working applied force), the following procedure was adopted. To make an initial estimate of the target value of F_{tip} to be used in the experiments, equation (1) was used with an AFM tip radius based on direct (SEM) observation, an indentation depth of 2 nm (the suppliers recommended minimum value), a modulus value taken from IIT for the stiffest polymer to be investigated (PMMA, 3.7 GPa) and with F_{adh} taken as zero. These calculated values are shown in table 2. An experiment was then run on the PS reference sample using the calculated target value of F_{tip}. Then, using the measured experimental parameters (F_{adh} and d), the AFM tip radius was recalculated so that the new E_r value was in agreement with the IIT value for PS.

The method described above gives a set of test parameters, which give the correct modulus for the PS reference sample but are not necessarily applicable to other samples. Hence, a second reference sample, photostress coating 1 (PS1) was used in order to refine the parameters. An iterative procedure was then adopted whereby a sample of PS1 was tested and F_{tip} was adjusted until the modulus matched the IIT value. The adjusted F_{tip} was then applied to the PS sample and the radius was again modified until the modulus matched the IIT value. The iterative process was continued until the values of F_{tip} and R, which produced an exact match for PS with respect to the IIT value, gave a mean modulus of PS1 that was within ±1 standard deviation of the IIT value. Following this calibration process, the working applied force and working radii were used for all the AFM measurements of the remaining polymers. These final values are shown in table 2.

3. Results

3.1. Introduction

This section describes Young's moduli results obtained by AFM nanomechanical mapping. Firstly, the implementation of the calibration procedure for each probe using the reference samples (PS and PS1) is described. Secondly, analytical predictions of the cantilever sensitivity are reported based on the experimental parameters presented in table 2. Finally, the results of Young's moduli measurements using the polymers listed in table 1 are presented.

3.2. Calibration

To establish the values for the working applied force (F_{tip}) and working radius (R), measurements were performed on both the PS and PS1 samples as described in the previous section. Young's moduli measurements after the calibration procedure had been completed for each probe are shown as histograms in figure 2 and a normal distribution of Young's moduli for each material can be seen. It seems reasonable that a distribution of Young's moduli would be measured due to the effect of polymer chain orientation and semi-crystallinity at the nanoscale. From these data, the mean and associated standard deviations were calculated and these values are shown in figure 3 plotted against Young's moduli measured using IIT.

As indicated above, figure 3 shows a comparison between the results of AFM and IIT nanomechanical mapping for the PS and PS1 calibration samples. As explained in the previous section, the calibration procedure resulted necessarily in agreement between the AFM nanomechanical mapping and

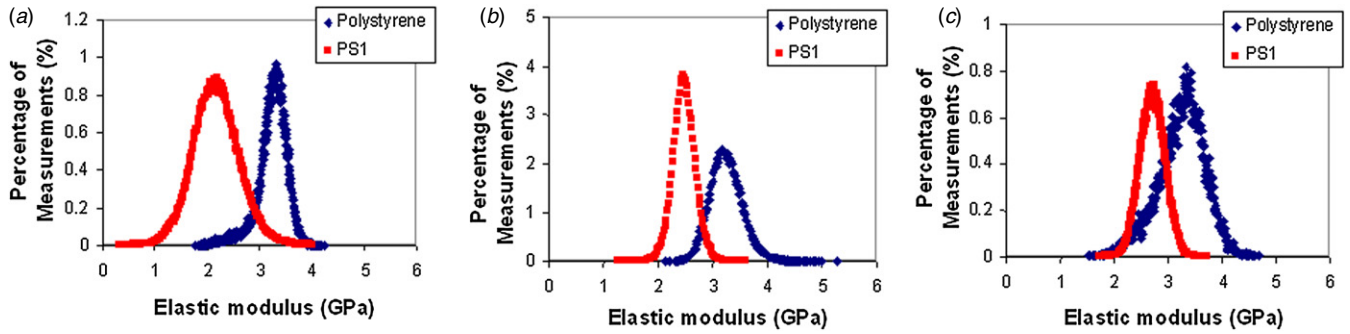

Figure 2. Histograms of Young's modulus measurements of PS and PS1 using (*a*) the Tap525 AFM probe, (*b*) the PDNISP AFM probe and (*c*) the Tap190 AFM probe.

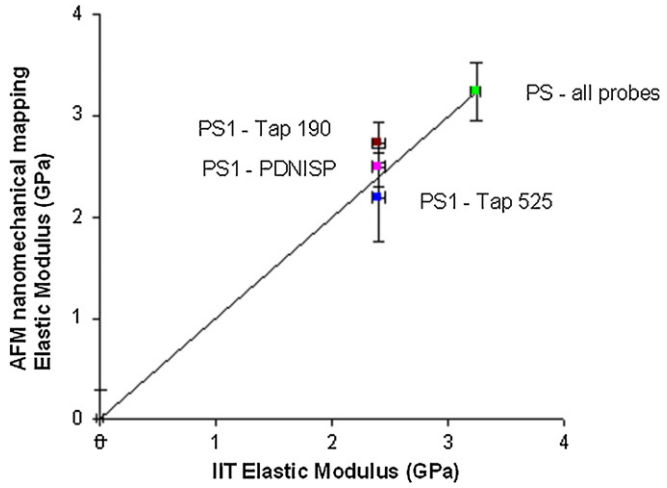

Figure 3. Comparison between Young's modulus measurements from IIT and AFM nanomechanical mapping using the three different AFM probes for the two reference samples: PS1 and PS.

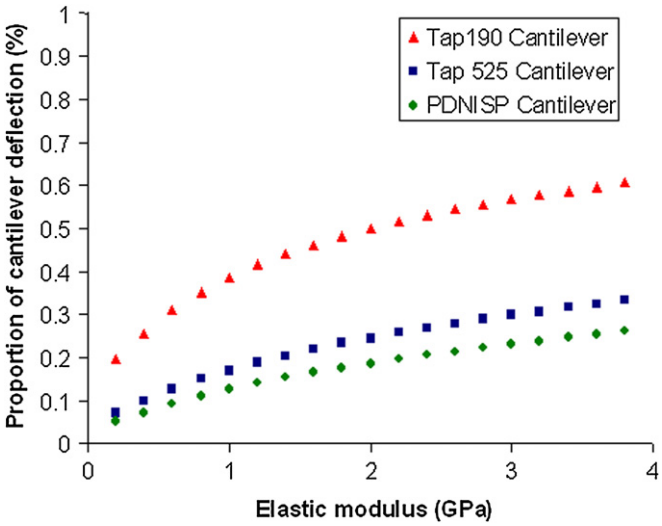

Figure 4. Calculated proportion of cantilever deformation for each AFM probe at the applied force as a function of surface Young's modulus—the total deformation is the sum of the sample and cantilever deformation.

IIT measurements for PS. The best agreement between the two techniques for PS1 was for the PDNISP probe, possibly because the tip apex was the most spherical and therefore had the best fit with the DMT model used to calculate Young's modulus. Figure 3 also shows that the Tap525 and the Tap190 have either slightly underestimated or overestimated, respectively, Young's modulus of PS1. However, in each case, the AFM nanomechanical measured Young's modulus of PS1 was within a standard deviation of the IIT measurement and so it was assumed that the experimental settings for each probe were reasonable for characterizing the remaining polymer surfaces.

3.3. Correlation of the cantilever sensitivity with Young's moduli variation

The suitability of each probe for measuring Young's moduli was determined by assessing the proportion of cantilever deflection to sample deformation. If the cantilever does not deflect when pressed against the surface because the cantilever stiffness is too high, it is not possible to measure the applied force or calculate the surface deformation. In contrast, if the cantilever deflects but there is no surface deformation because the cantilever stiffness is too low, then any error in the cantilever deflection measurement could be misinterpreted as sample deformation. For this reason, the proportion of cantilever deflection is indicative of how sensitive any particular probe is when measuring surfaces within a given stiffness range. For each of the three AFM probes used in this study, the proportion of the deflection ascribed to the cantilever and the sample were calculated for each of the test polymers using equation (3):

$$d_{\text{total}} = d_{\text{cantilever}} + d_{\text{sample}} = \underbrace{\left(\frac{F_{\text{tip}}}{k}\right)}_{\text{Cantilever deformation}} + \underbrace{\left(\frac{3F_{\text{tip}}}{4E^{*}\sqrt{R}}\right)^{\frac{2}{3}}}_{\text{Sample deformation}}. \tag{3}$$

Figure 4 shows the predicted percentage of cantilever deformation (as a proportion of total deflection) with increasing sample Young's modulus for each probe. The Tap190 probe has the largest proportion of cantilever deflection out of the three AFM probes, which indicates that it may provide the most sensitive measurement. In contrast, the PDNISP probe (with a relatively high stiffness) will deflect the least and hence it may not be possible to detect the first point of contact for the less stiff polymers.

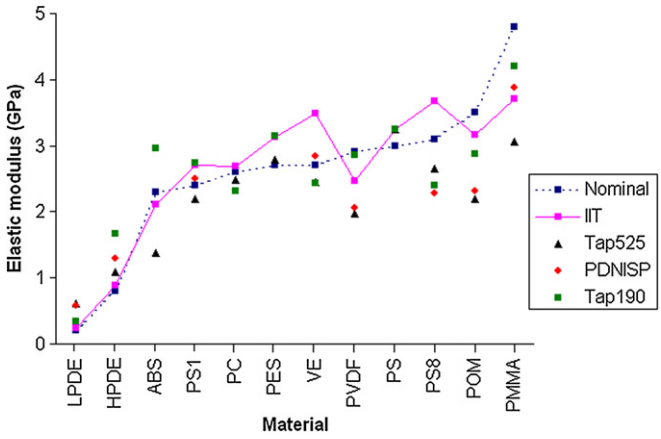

Figure 5. Young's moduli values for 12 polymers obtained from suppliers (nominal) by IIT and by AFM nanomechanical mapping using the three different AFM probes.

Table 3. Measured values of average Young's moduli and standard deviations obtained for the polymeric surfaces by quantitative nanomechanical mapping and IIT.

	Young's moduli values (GPa) and standard deviation			
	IIT	Tap525	PDNISP	Tap190
LDPE	0.24 ± 0.001	0.62 ± 0.16	0.58 ± 0.10	0.34 ± 0.08
HDPE	0.88 ± 0.001	1.08 ± 0.24	1.30 ± 0.26	1.67 ± 0.33
ABS	2.11 ± 0.05	1.38 ± 0.48		2.96 ± 1.17
PS1	2.70 ± 0.06	2.19 ± 0.44	2.50 ± 0.19	2.73 ± 0.20
PC	2.68 ± 0.001	2.49 ± 0.26		2.31 ± 0.19
PES	3.12 ± 0.04	2.78 ± 0.18		3.15 ± 0.18
VE	3.49 ± 0.02	2.45 ± 0.53	2.84 ± 0.40	2.42 ± 1.00
PVDF	2.46 ± 0.05	1.98 ± 0.45	2.06 ± 0.35	2.86 ± 0.36
PS	3.24 ± 0.03	3.24 ± 0.29	3.24 ± 0.29	3.24 ± 0.39
PS8	3.67 ± 0.04	2.65 ± 0.60	2.28 ± 0.24	2.39 ± 0.17
POM	3.17 ± 0.16	2.19 ± 0.44	2.32 ± 0.23	2.88 ± 0.57
PMMA	3.70 ± 0.02	3.06 ± 0.58	3.88 ± 0.63	4.20 ± 1.36

3.4. Results of quantitative nanomechanical measurement of polymers

Figure 5 shows comparisons between the average Young's moduli measured by IIT, the nominal value provided by the suppliers for the various polymer surfaces and the AFM nanomechanical mapping results (for each of the three AFM probes). Overall, the AFM average values of Young's moduli are similar to the IIT and the suppliers' values. The best agreement is for polymers that have Young's moduli between that of the two reference samples, PS1 and PS. Outside of this range, the AFM nanomechanical mapping technique tended to measure higher Young's moduli for the softer polymers and lower Young's moduli for the harder polymers, in relation to the suppliers' or IIT values. This is not unexpected, given that the calibration procedure optimized the control variables F_{tip} and R for polymers having a stiffness between that of PS1 and PS.

Table 3 shows the average values of the measured Young's moduli and the associated standard deviations obtained for each polymer surface using IIT and AFM nanomechanical mapping. Although the results obtained by AFM nanomechanical mapping show a much lower precision (i.e. a higher standard deviation) than the IIT values, there are very many measurements made for each modulus measurement (over 65 000), thus giving a high confidence in the average modulus measurement, assuming there are no systematic errors in the results. In contrast, the indentation results obtained by IIT have a lower standard deviation. The variation in the measured Young's moduli and associated standard deviations between the two test techniques may be attributed to the difference in the indentation depths and sampled volume, the mechanical model assumed and the tip profiles. The AFM nanomechanical mapping technique is designed to measure Young's modulus of a surface with as little as 2 nm sample deformation. In contrast, measurement of Young's modulus of polymers by IIT involves indentation depths of tens of nanometres. In addition to the length scale, the mathematical model and tip profile are also different. The results obtained by AFM nanomechanical mapping are modelled using a DMT model, which is for Young's contact using a spherical indenter, whereas IIT is modelled using an Oliver and Pharr model designed for the elastic–plastic contact using a Berkovich indenter. In summary, therefore, the AFM may be considered to be a tool suitable for the detection of local mechanical properties, rather than overall bulk material properties.

The measured average Young's moduli values are generally similar for the Tap525 and PDNISP probes (see table 2), which is likely to be a result of the similarities in the probe geometries (see table 2) and the proportion of cantilever deformation (see figure 4) for the two AFM probes. In general, the PDNISP probe shows the smallest standard deviation for the measured samples, perhaps suggesting that a small proportion of cantilever deflection leads to more precise Young's moduli measurements. However, it should be noted that it was not possible to measure the modulus for some of the polymers using the PDNISP probe (see table 2). This may be associated with the higher applied force for the PDNISP probe, which in turn leads to higher friction, and different rate-dependent responses for the various polymers. It should be noted that it is not possible to change the indentation displacement rate within the nanomechanical test by more than a factor of 2.

4. Concluding remarks

This work has shown that AFM nanomechanical mapping has the potential to be a useful supplement (with higher spatial resolution and surface sensitivity) to IIT for measuring the small-scale Young's modulus of a polymer surface. The technique can provide repeatable measurements of polymer moduli for a number of different probes when careful calibration procedures are used. In spite of this, there are difficulties when polymer surfaces are characterized that have significantly different moduli from the calibration samples, which might partially be overcome if the PeakForce^{TM} QNM^{TM} software could be modified to allow for additional contact models to be used in the analysis.

Acknowledgments

This work was supported by the National Physical Laboratory as part of a Department for Business, Innovation and Skills (BIS)-funded project and an Engineering and Physical Sciences Research Council (EPSRC)-funded Engineering Doctorate.

References

[1] Binnig G and Quate C F 1986 Atomic force microscope *Phys. Rev. Lett.* **56** 930–3
[2] Binnig G, Gerber C, Stoll E, Albrecht T R and Quate C F 1987 Atomic resolution with atomic force microscope *Europhys. Lett.* **3** 1281–6
[3] Maivald P *et al* 1991 Using force modulation to image surface elasticities with the atomic force microscope *Nanotechnology* **2** 103
[4] Magonov S, Elings V and Whangbo M 1997 Phase imaging and stiffness in tapping-mode atomic force microscopy *Surf. Sci.* **375** L385–91
[5] Burnham N A 1989 Measuring the nanomechanical properties and surface forces of materials using an atomic force microscope *J. Vac. Sci. Technol.* A **7** 2906
[6] Rosa-Zeiser A, Weilandt E, Hild S and Marti O 1997 The simultaneous measurement of elastic, electrostatic and adhesive properties by scanning force microscopy: pulsed-force mode operation *Meas. Sci. Technol.* **8** 1333
[7] VanLandingham M R, McKnight S H, Palmese G R, Eduljee R F, Gillespie J W and McCulough J R 1997 Relating elastic modulus to indentation response using atomic force microscopy *J. Mater. Sci. Lett.* **16** 117–9
[8] Pittenger B, Erina N and Su C 2010 Quantitative mechanical property mapping at the nanoscale with PeakForce QNM http://nanoscaleworld.bruker-axs.com/nanoscaleworld/media/p/418.aspx
[9] Sahin O, Magonov S, Su C, Quate C F and Solgaard O 2007 An atomic force microscope tip designed to measure time-varying nanomechanical forces *Nat. Nanotechnol.* **2** 507–14
[10] Lin D C, Dimitriadis E K and Horkay F 2007 Robust Strategies for automated AFM force curve analysis: II. Adhesion-influenced indentation of soft, elastic materials *J. Biomech. Eng.* **129** 904
[11] Vanlandingham M R *et al* 1997 Nanoscale indentation of polymer systems using the atomic force microscope *J. Adhes.* **64** 31–59
[12] Richter F *et al* 2006 Substrate influence in Young's modulus determination of thin films by indentation methods: cubic boron nitride as an example *Surf. Coat. Technol.* **201** 3577–87
[13] Vandamme M and Ulm F 2006 Viscoelastic solutions for conical indentation *Int. J. Solids Struct.* **43** 3142–65
[14] Derjaguin B 1975 Effect of contact deformations on the adhesion of particles *J. Colloid Interface Sci.* **53** 314–26
[15] Clifford C A and Seah M P 2005 Quantification issues in the identification of nanoscale regions of homopolymers using modulus measurement via AFM nanoindentation *Appl. Surf. Sci.* **252** 1915–33